Am J Transl Res 2019;11(6):3531-3542
www.ajtr.org /ISSN:1943-8141/AJTR0092766

*Original Article*

# Loquat leaf polysaccharides improve glomerular injury in rats with anti-Thy 1 nephritis via peroxisome proliferator-activated receptor alpha pathway

Ting Lu[1*], Zhimin Fan[2*], Jianhao Hou[1], Xiaohong Qi[3], Mengjie Guo[1], Jianming Ju[4], Ye Yang[1,5], Chunyan Gu[1,2]

*[1]School of Medicine and Life Sciences, Nanjing University of Chinese Medicine, Nanjing 210023, China; [2]The Third Affiliated Hospital of Nanjing University of Chinese Medicine, Nanjing 210001, China; [3]Department of Pathophysiology, Nanjing Medical University, Nanjing 211166, China; [4]Affiliated Hospital of Integrated Traditional Chinese and Western Medicine, Nanjing University of Chinese Medicine, Nanjing, China; [5]School of Holistic Integrative Medicine, Nanjing University of Chinese Medicine, Nanjing 210023, China. [*]Equal contributors.*

Received February 19, 2019; Accepted May 6, 2019; Epub June 15, 2019; Published June 30, 2019

**Abstract:** Chronic glomerulonephritis frequently develops into renal failure that cannot be completely cured. Based on the success of anti-inflammatory Chinese herbs in treating chronic nephritis, our goal was to investigate the therapeutic effects and mechanism of action of loquat leaf polysaccharides (LLPS) on chronic anti-Thy-1 nephritis. A rat model of glomerulonephritis was used to study the effects of 8 weeks of enalapril or LLPS treatment. Twenty-four-hour rat urinary protein excretions were measured every week for 8 weeks. Then, all animals were sacrificed, renal-related biochemical parameters were analyzed, and histology and electron microscopy examinations of renal tissue samples were conducted. Renal cortex tissue was used to detect markers of renal fibrosis. RNA sequencing (RNA-seq) and *in vitro* experiments explored the signaling pathway involved in LLPS treatment effects. Compared with the disease control group, LLPS treatment significantly decreased the levels of serum creatinine and blood urea nitrogen, reduced urinary protein excretion, glomerular mesangial cell proliferation, and extracellular matrix hyperplasia, and attenuated the expression of proteins associated with podocyte injury and renal fibrosis. RNA-seq results showed that peroxisome proliferator-activated receptor (PPAR) is a potential signaling pathway involved in LLPS treatment of chronic glomerulonephritis. Increases in PPARα and plasminogen activator inhibitor-1 (PAI-1) caused by glomerulonephritis were inhibited by LLPS *in vitro*. Furthermore, when an agonist of PPARα (BMS-687453) was used to stimulate PPARα activity, LLPS treatment suppressed the expression of fibrosis factor PAI-1 partially via PPARα inhibition. These findings demonstrate that LLPS improved glomerular injury in rats with anti-Thy 1 nephritis via the PPARα pathway.

**Keywords:** Loquat leaf polysaccharides, glomerulonephritis, renal fibrosis, PPARα signaling pathway

## Introduction

Chronic kidney disease (CKD) is a worldwide health problem [1] that is characterized by progressive destruction of renal parenchyma and loss of functional nephrons, which ultimately lead to end-stage renal failure [2-4]. CKD is secondary to renal fibrogenesis, which is characterized by abnormal deposition of extracellular matrix (ECM), collagen, and elastic fibers [5-7]. Glomerular fibrosis, which causes glomerulosclerosis [8], and tubulointerstitial fibrosis, which leads to the decline of renal filtration function [9], eventually result in the rapid progression of chronic nephropathy [10]. Podocyte injury is crucial in the pathogenesis of glomerular disease, with proteinuria leading to CKD [11-13]. Clinical evidence has proven that angiotensin-converting enzyme inhibitors and angiotensin receptor blockers can lower blood pressure, decrease proteinuria, and retard CKD progression. However, not every CKD patient has a good outcome, especially non-dialysis patients with stage 5 CKD or patients with hyperkalemia or acute kidney injury [2, 14].

Several Chinese medicines, such as Shen-Kang and Rhubarb, have been proven to be effective in treating chronic nephritis [15, 16]. Various traditional Chinese medicine extracts, including

general acteoside of rehmanniae leaves and multi-glycoside of *Tripterygium wilfordii Hook. f.*, are also prescribed for chronic nephritis patients [17-19]. Dihydroartemisinin has also been applied to treat glomerular disease with mesangial cell proliferation [20]. Nonetheless, there is little literature on the treatment of polysaccharides in chronic nephritis. Compelling evidence has indicated that loquat leaf exerts potent inhibitory effects on inflammatory mediators, including nitric oxide, inducible nitrous oxide synthase, cyclooxygenase-2, tumor necrosis factor-α, and interleukin-6, via attenuation of the nuclear factor kappa-light-chain enhancer of activated B cells (NF-κB) translocation to the nucleus [21]. It has also been reported that the extract of loquat leaf possesses the ability to inhibit the activation of many inflammation-related genes and inflammatory mediators [22] and may be used as an anti-inflammatory and analgesic agent for treating pain and inflammatory diseases [23]. Polysaccharides, such as astragalus polysaccharide [24] and polysaccharides from *Irpex lacteus* (Fr.) Fr. [25], have attracted attention as a treatment for glomerulonephritis that acts by inhibiting the NF-κB pathway or exhibiting anti-inflammatory action. However, the therapeutic effect of loquat leaf polysaccharides (LLPS) on chronic glomerulonephritis has not been investigated.

In this study, we used anti-Thy 1 rats, a well-established rodent model of nephritis, to evaluate the effect of LLPS on experimental glomerulonephritis and to explore the potential signaling pathway.

## Materials and methods

### *Reagents*

The LLPS (provided by Prof. Ju) were extracted from loquat leaf by water extraction and alcohol precipitation, and proteins were removed by the Sevag method [26-29]. Loquat leaf (500 g) was extracted with 5 L of water two times for 1.5 h and a third time for 1 h. The water extracts (approximately 16 L) were combined, filtered, and evaporated to 500 mL by rotary evaporation under vacuum. Then, 95% ethanol was slowly added into the concentrated solution with constant stirring to achieve an ethanol concentration of 80%. After the solution was allowed to stand for 12 h, the supernatant was removed and the lower layer precipitate was centrifuged at 4500 rpm for 15 min. The precipitate was washed three times with absolute ethanol and dried under vacuum. In total, 43 g of crude polysaccharide was obtained and then dissolved in distilled water to yield a solution with a final volume of 1 L. Trichloroacetic acid (10%) was added to the solution in a 3:1 ratio of polysaccharide to trichloroacetic acid. After 6 h at rest, the mixture was centrifuged at 4500 rpm for 15 min to remove proteins, and the pH of supernatant was adjusted to 7. After the supernatant was concentrated to 600 mL, 95% ethanol was added with constant stirring to keep the ethanol concentration at 80%. After standing for 12 h, the lower layer precipitate was centrifuged at 4500 r/min for 15 min, washed three times with absolute ethanol, and dried under vacuum at 75°C. After grinding, 25 g of deproteinized LLPS was obtained (Drug material: Jingui loquat leaf; Place of origin: Sichuan; Production date: July 7, 2015).

Enalapril was obtained from SZYY Group Pharmaceutical Limited (Jiangsu, China). All other materials and chemicals, unless otherwise indicated, were obtained from Sigma Chemical Co. (St. Louis, MO, USA).

### *Animals*

Male Sprague-Dawley rats (200±20 g) were purchased from Beijing Vital River Laboratory Animal Technology Co., Ltd. All animal procedures were in accordance with government-published recommendations for the Care and Use of Laboratory Animals. The animal study was approved by the Institutional Ethics Review Boards of Nanjing University of Chinese Medicine (Ethics number ACU-14 (20151123)).

### *Experimental groups*

Twenty-eight male Sprague-Dawley rats were randomly assigned to four groups: normal control group (NC), disease control group (DC), enalapril (Ena) group (positive group, which is widely used to cure chronic kidney failure [30]), and LLPS group. The rat anti-Thy 1 nephritis model was established by tail vein injection of rabbit anti-rat thymocyte serum (1.75 mg/kg body weight). NC animals were injected with equal volumes of phosphate-buffered saline only. After 1 week, the rats were treated with an oral gavage of Ena or LLPS once daily for 8 weeks, while rats in NC group and DC group were given equal volumes of water.

*Measurement of renal function parameters*

Urine samples were collected from rats housed in metabolic cages for 24 h once a week after injecting anti-Thy1 serum (ATS). After 8 weeks of treatment, the rats were anesthetized, and blood was immediately collected from the abdominal aorta. Blood urea nitrogen (BUN), creatinine (Cr) levels, and calculated creatinine clearance ratio (Ccr) serve as markers of renal function. The urinary protein excretion was measured using a Pierce™ BCA Protein Assay Kit (Thermo Fisher Scientific, Waltham, MA, USA). Urine Cr was measured using a QuantiChrom™ Creatinine Assay Kit (Bio Assay System, Hayward, CA, USA) for the calculation of Ccr. Plasma BUN and Cr levels were determined by standard laboratory procedures. The Ccr [31] was calculated using the following formula: (Urine Cr levels/plasma Cr levels) • 24 • Urine volume (mL)/(24 h × 60 min).

*Cell culture*

Murine mesangial cells (MMCs) were provided free by Nanjing Key Laboratory of Pediatrics. The MMCs were cultured at 37°C in a humidified 5% $CO_2$ atmosphere and passaged every 2-3 days in 100-mm dishes containing DMEM with low glucose supplemented with 10% fetal bovine serum, 100 U/mL penicillin, and 100 μg/mL streptomycin. After several days of adaptive culture, the MMCs were divided into groups cultured with low-glucose medium (5.6 mM) and high-glucose medium (25 mM) [32]. High-glucose culture promotes proliferation of mesangial cells, inflammatory factor, and collagen accumulation [33-35]. The high-glucose medium group was randomly divided into the high-glucose group, the LLPS group, the BMS-687453 group, and the LLPS+BMS-687453 group. After intervention for 48 h, the total protein was extracted for western blot analysis.

*Histological analyses*

*Electron microscopy:* Kidney tissue was removed from the abdominal cavity of the rats and divided into several parts. The renal cortex was fixed with 2.5% glutaraldehyde and sliced into ultrathin sections for electron microscopy analysis. The images were captured using a transmission electron microscope (Tecnai G2 Spirit Bio TWIN). Ultrastructural changes of glomerular basement membrane and glomerular podocytes were observed by electron microscopy.

*Periodic Acid-Schiff (PAS) staining:* Renal cortex tissues were fixed in 10% neutral formalin for 24 h and then embedded in paraffin. The embedded tissues were cut into 3-μm-thick sections for morphological analysis by PAS staining. Glomerular mesangial expansion was determined in 20 glomeruli per slide in a blinded manner. The images of random glomeruli were captured using an Axio VertA 1 digital camera, and the area of PAS-positive glomeruli was quantified using a computer-assisted color image analysis system (Image J). The extent of glomerular matrix expansion was assessed in a relative value according to area of positive staining field. Scores were calculated on a 0-4 scale (0: 0%, 1: 1-25%, 2: 26-50%, 3: 51-75%, and 4: 76-100%).

*Western blot analysis*

Renal tissues stored at -80°C or cell precipitations were lysed in RIPA lysis buffer with protease inhibitor cocktail, and protein concentration was detected using a BCA Protein Assay kit (Thermo Fisher, New York, NY, USA). Total tissue or cell lysate mixed with sample buffer and β-mercaptoethanol (equal to 20 μg of protein) was fractionated by SDS-PAGE on a 10% polyacrylamide gel and transferred to polyvinylidene fluoride (PVDF) membranes. After being blocked with 5% non-fat milk, membranes were incubated overnight with primary antibody (diluted 1:1,000) at 4°C. The following primary antibodies were used: rabbit polyclonal WT1 antibody (sc-192, diluted 1:1,000; Santa Cruz Biotechnology), rabbit polyclonal plasminogen activator inhibitor-1 (PAI-1) antibody (ab66705, diluted 1:1,000; Abcam), rabbit polyclonal peroxisome proliferator-activated receptor alpha (PPARα) antibody (15540-1-AP, diluted 1:1,000; Proteintech). The rabbit polyclonal β-actin antibody (#4967, diluted 1:1,000; Cell Signaling Technology) served as loading controls. After being washed with TBST (mixture of tris-buffered saline and Tween 20), the blots were incubated in goat anti-rabbit horse radish peroxidase (HRP)-conjugate antibody (sc-2004, diluted 1:10,000; Santa Cruz Biotechnology) for 1 h at room temperature [36]. Proteins were visualized with the Tannon™ High-sig ECL Western Blotting Substrate (Tannon, Shanghai, China).

*Transcriptiomic RNA sequencing*

The RNA-seq and sample analysis were performed by Xinyinzi Bio-tech (Shanghai, China). Briefly, mRNA was extracted from the total RNA

**Table 1.** Renal function of experimental rats

| Renal Function | NC | DC | Ena | LLPS |
|---|---|---|---|---|
| Plasma BUN (mmol/L) | 5.31±0.16 | 8.53±1.67* | 6.01±0.74# | 6.10±0.21# |
| Plasma Cr (μmol/L) | 29.5±0.93 | 37.33±2.07* | 35.83±4.31 | 36.17±4.22* |
| Ccr (mL/min) | 2.38±0.93 | 1.32±0.57* | 2.04±0.94 | 1.99±0.93 |

NC: normal control; DC: disease control; Ena: enalapril (10 mg/kg/d); LLPS: Loquat leaf polysaccharides (100 mg/kg/d); *P<0.05 vs NC; #P<0.05 vs DC.

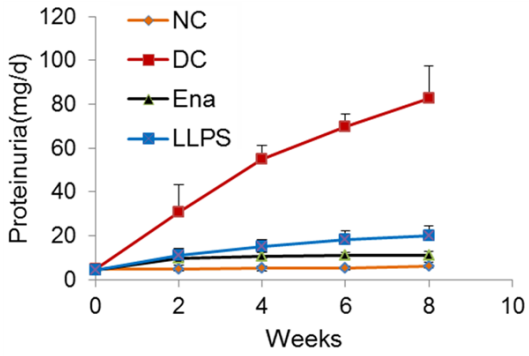


| *P* value | NC | DC | Ena | LLPS |
|---|---|---|---|---|
| vs NC | | 0.01 | 0.014986 | 0.014613 |
| vs DC | | | 0.023191 | 0.04076 |

**Figure 1.** Twenty-four-hour urinary protein excretion in rats with anti-Thy 1 nephritis. Significant differences among groups are shown in detail with *P* values.

of cortex tissues after removing the rRNA. This project used *Rattus_norvegicus* ref RNA-seq data sequencing and an analysis technology service. After constructing an RNA sequencing library, Hi Seq X-Ten was utilized for PE150 sequencing. Data were analyzed using strict data quality control, and differentially expressed genes were found.

*Statistical analysis*

Results are shown as mean ± standard deviation (SD). Significant differences among groups were analyzed by one-way ANOVA or paired t-test using SPSS 22.0 software. A *P* value of <0.05 was considered significant.

## Results

*LLPS improved the renal function of rats with anti-Thy 1 nephritis*

The levels of plasma BUN and Cr were significantly increased in the rats with disease induced by the administration of ATS, and the Ccr levels were decreased in the DC group compared to the NC group. Plasma BUN of LLPS-treated rats was reduced by 28%, which was significantly lower than that in disease animals. The Cr levels in the LLPS treatment group were elevated, but did not reach statistical significance (**Table 1**). The 24 h proteinuria in the DC group rats was significantly increased after ATS injection and continued to rise during the following 8 weeks. LLPS treatment resulted in obvious reduction of 24-h proteinuria by 76% compared to that in DC group (**Figure 1**).

*LLPS ameliorated glomerular damage observed by electron microscope*

The glomerular structures, including the podocytes, were well maintained in the control samples. Compared with the NC group, the DC group showed typical signs of mesangial cells proliferation, mesangial matrix hyperplasia, irregular basement membrane thickening, and fusion of foot processes, all of which indicated glomerular damage. Both groups of rats treated with LLPS or Ena presented with reduction of mesangial cell proliferation, improvement of glomerular basement membrane thickening and decrease of foot process fusion (**Figure 2A**). As summarized in **Figure 2B** and **2C**, the glomerular basement membrane thickness and foot processes width showed significant decreases (P<0.05) in rats treated with either Ena or LLPS compared to DC animals (**Figure 2B** and **2C**). The expression of a nucleoprotein Wilms' tumor 1 (WT1), recognized as a podocyte-related biomarker [37, 38] specific to adult renal foot cells and parietal glomerular epithelial cells, was markedly reduced in the DC group. Similar to the Ena group, LLPS treatment also reversed the decreased WT1 expression (**Figure 2D**).

*LLPS attenuated renal fibrosis in rats with anti-Thy 1 nephritis*

In the nephritis model group, hyperplasia of mesangial cells was aggravated, followed by

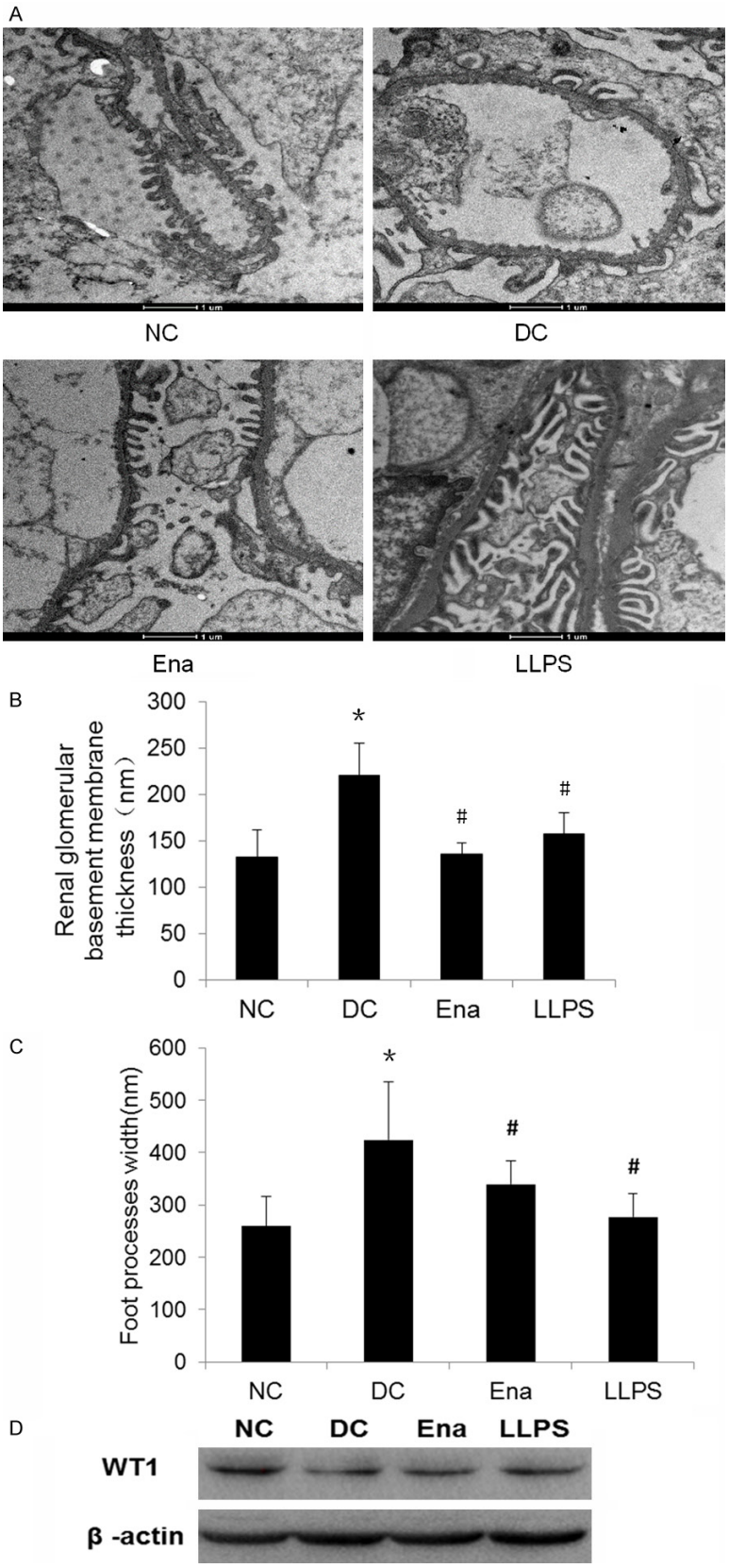


**Figure 2.** Effects of LLPS on improving podocyte injury in experimental animals. A. Pathological changes of renal cortex observed by electron microscopy (6800 ×). B. Scores of renal glomerular basement membrane thickness. C. Scores of foot processes width. D. Level of WT1 protein expression analyzed by western blot. Key: (*) P<0.05 vs NC; (#) P<0.05 vs DC.

stenosis or even occlusion of capillary cavities. Focal segmental scleroses were found in some glomeruli, presenting as increments of glomerular mesangial matrices and thickening of the renal capsule wall. Representative glomeruli of PAS staining are shown in **Figure 3A**. The glomeruli in the DC group showed remarkable accumulation of ECM compared to normal glomeruli. Both LLPS and Ena caused progressive reduction in glomerular matrix accumulation. As shown in **Figure 3B**, a significant decrease in PAS staining was seen in rats treated with either LLPS or Ena compared to DC rats (P<0.05). PAI-1, which is thought to decrease the reversal of the pathological ECM and is associated with renal fibrosis [39], was significantly up-regulated in the DC group. Conversely, LLPS treatment attenuated the expression of PAI-1 protein (**Figure 3C**).

Taken together, these data indicate that LLPS treatment could protect kidney function, inhibit ECM accumulation, and ameliorate glomerular damage in experimental anti-Thy1 nephritis.

*RNA-seq analyses revealed the potential signaling pathway involved in LLPS treatment in chronic glomerulonephritis*

We also sought to determine the mechanism of the LLPS protective effect on kidney function in anti-Thy1 nephritis. An RNA-seq analysis was

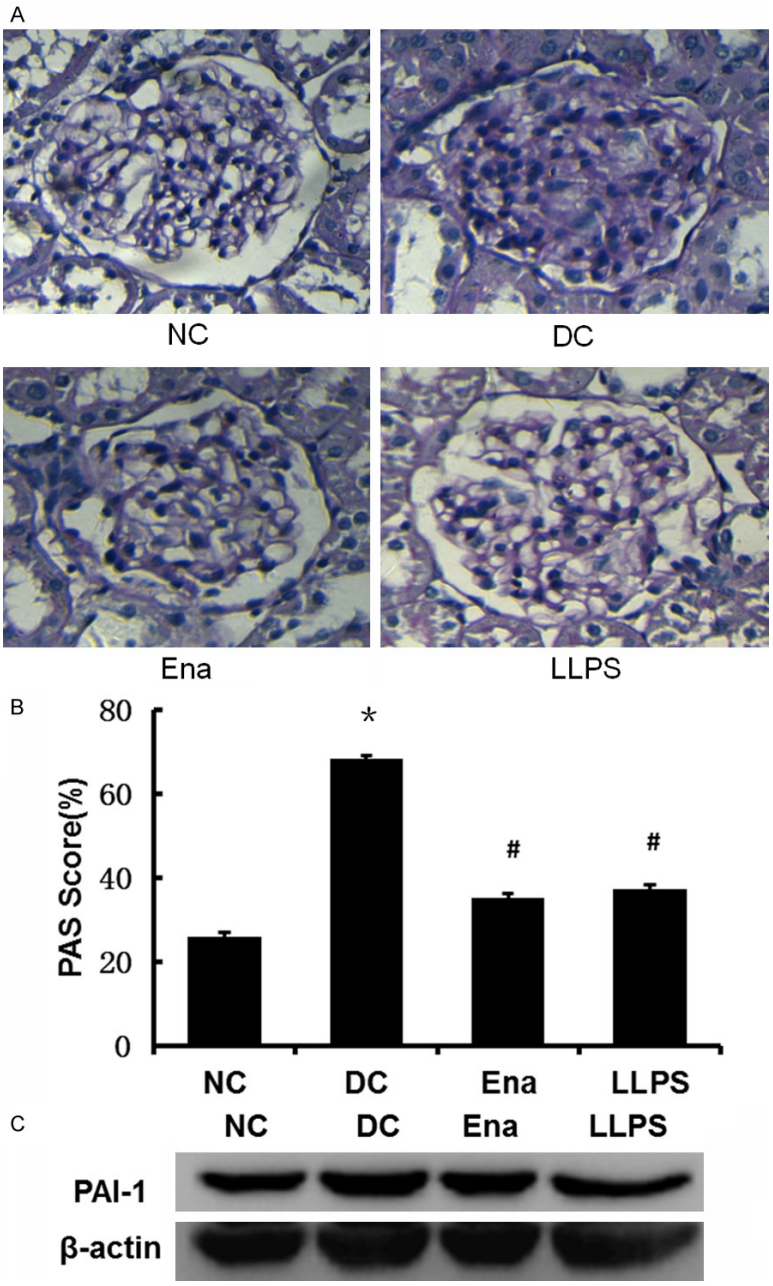


**Figure 3.** Effects of LLPS on improving renal fibrosis in experimental animals. A. Glomeruli of kidney stained with periodic acid-Schiff stain (PAS) (400 ×). B. The score of the glomerular extracellular matrix. C. The level of PAI-1 protein expression analyzed by western blot. Key: (*) P<0.05 vs NC; (#) P<0.05 vs DC.

performed to detect differential expression profiles in the renal cortex of NC, DC, and LLPS groups. In total, 504 up-regulated genes and 297 down-regulated genes were significantly differentially expressed between the LLPS and DC groups (|FoldChange| ≥2, *P* value ≤0.05 (**Figure 4A**)). The Venn diagram in **Figure 4B** shows that 20 differentially expressed genes were significantly altered in all three sample types; namely, Atp5me, Prodh1, Acacb, Mid-1ip1, Cyp7a1, Nampt, Gadd-45g, Rps14, Hacl1, Hes6, Arrdc3, Mup, Hspa1a, G6pc, AC123346.1, Pemt, AABR0-7066188.1, Igfbp1, Gck, and a novel gene. Representative gene ontology (GO) Biological Process terms and KEGG pathways selected from the most enriched charts are shown in **Figure 4C** and **4D**. Predicted genes were categorized into three ontologies: biological process (BP), cellular component (CC), and molecular function (MF). The significantly enriched GO terms with more numbers of genes for BP, CC, and MF (**Figure 4C**) were related to organelle and catalytic activity metabolic processes, respectively. Corresponding pathways were analyzed by KEGG analysis. Only the top 20 most significantly enriched pathways are shown in **Figure 4D**. Based on the identified mRNA regulations, the PPAR signaling pathway was found to be one of the most significantly enriched pathways.

*PPARα signaling pathway was validated by the in vitro experiment*

PPAR was selected as a potential signaling pathway based on the gene expression profile. PPARα is a member of PPARs, which are ligand-activated transcription factors of a nuclear hormone receptor superfamily [40]. Consistent with results of the gene expression profile, PPARα was easily detected by western blot in the cortex tissues of DC rats. In contrast, PPARα expression was evidently decreased in rats treated with LLPS (**Figure 5A**). To further confirm the role of the PPARα signaling pathway in the treatment of LLPS, cellular experiments were carried out. As

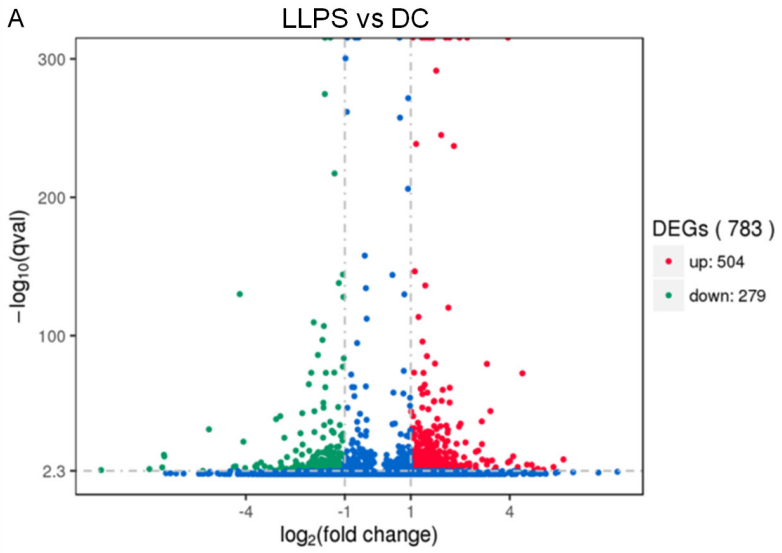
A
LLPS vs DC
300
200
100
2.3
−log10(qval)
-4
-1
1
4
log2(fold change)
DEGs ( 783 )
up: 504
down: 279

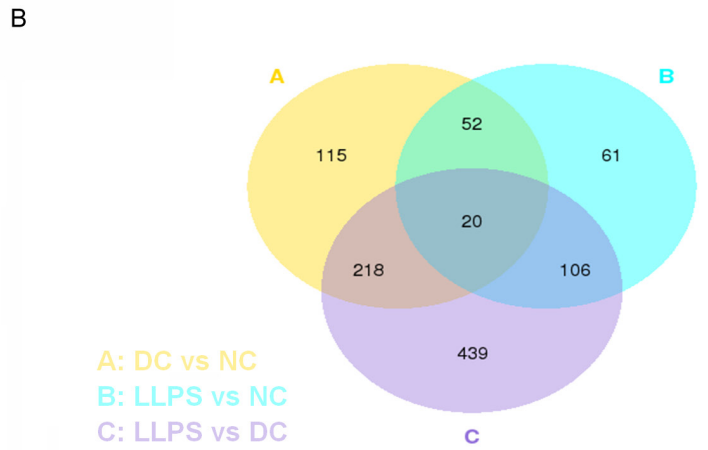
B
A
B
C
115
52
61
20
218
106
439
A: DC vs NC
B: LLPS vs NC
C: LLPS vs DC

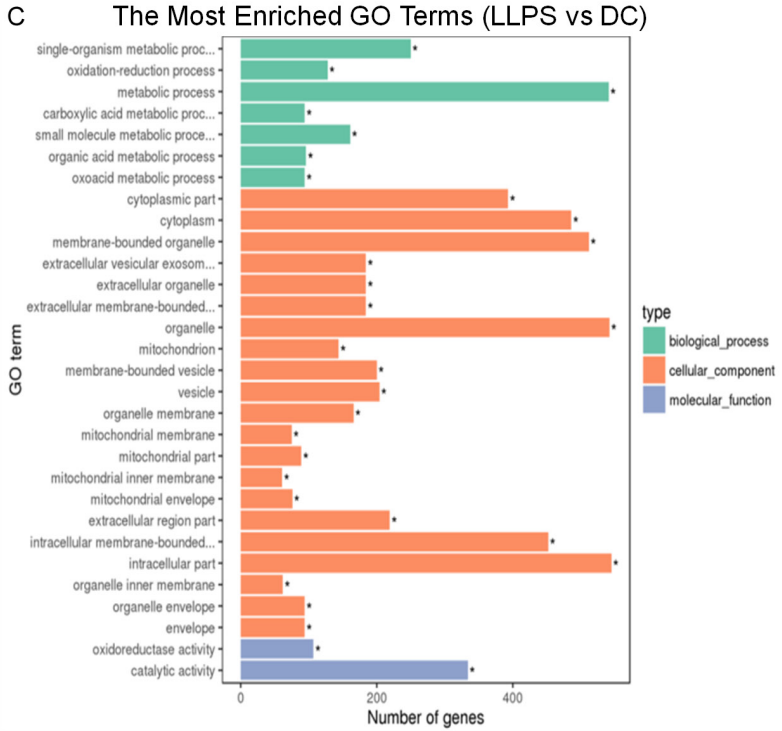
C
The Most Enriched GO Terms (LLPS vs DC)
single-organism metabolic proc...
oxidation-reduction process
metabolic process
carboxylic acid metabolic proc...
small molecule metabolic proce...
organic acid metabolic process
oxoacid metabolic process
cytoplasmic part
cytoplasm
membrane-bounded organelle
extracellular vesicular exosom...
extracellular organelle
extracellular membrane-bounded...
organelle
mitochondrion
membrane-bounded vesicle
vesicle
organelle membrane
mitochondrial membrane
mitochondrial part
mitochondrial inner membrane
mitochondrial envelope
extracellular region part
intracellular membrane-bounded...
intracellular part
organelle inner membrane
organelle envelope
envelope
oxidoreductase activity
catalytic activity
GO term
0
200
400
Number of genes
type
biological_process
cellular_component
molecular_function

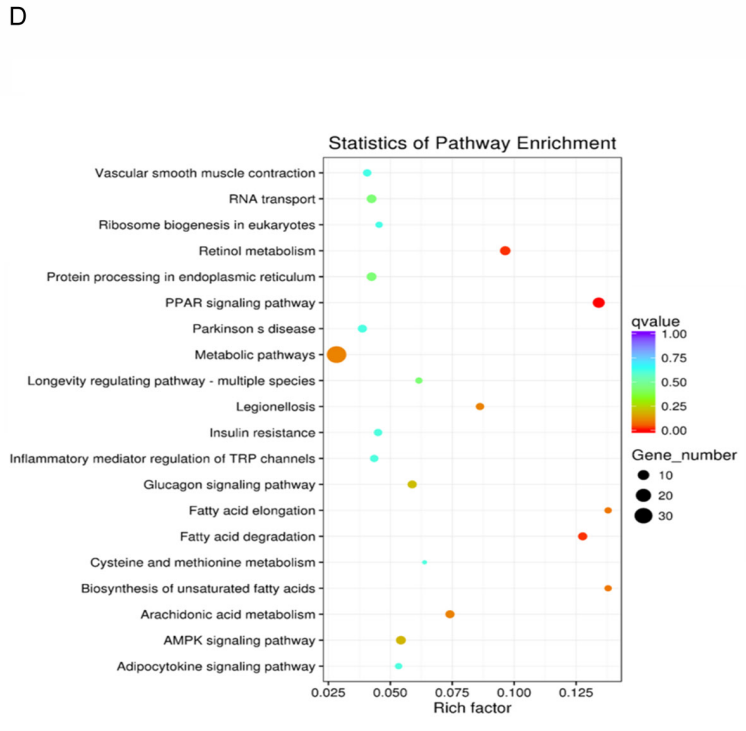
D
Statistics of Pathway Enrichment
Vascular smooth muscle contraction
RNA transport
Ribosome biogenesis in eukaryotes
Retinol metabolism
Protein processing in endoplasmic reticulum
PPAR signaling pathway
Parkinson s disease
Metabolic pathways
Longevity regulating pathway - multiple species
Legionellosis
Insulin resistance
Inflammatory mediator regulation of TRP channels
Glucagon signaling pathway
Fatty acid elongation
Fatty acid degradation
Cysteine and methionine metabolism
Biosynthesis of unsaturated fatty acids
Arachidonic acid metabolism
AMPK signaling pathway
Adipocytokine signaling pathway
0.025
0.050
0.075
0.100
0.125
Rich factor
qvalue
1.00
0.75
0.50
0.25
0.00
Gene_number
10
20
30

**Figure 4.** Large scale gene expression profiles. A. The volcano plot was used to enable visualization of the relationship between fold change and statistical significance. The red point in the plot represents up-regulated mRNA (fold change >2, P<0.05), the green point indicates down-regulated mRNA (fold change <2, P<0.05), and the blue point shows mRNA with no statistical difference (fold change <2, P>0.05). B. Venn diagram of differential expressed genes detected in the four different groups. The overlap represents 20 differentially expressed genes common to the three different groups. C. Gene ontology (GO) classification of target genes. The 30 most significantly enriched GO terms for the whole kidney. The x-axis represents the numbers of genes and the y-axis represents the diverse biological functions of target genes according to the three GO categories, including biological process, cellular component, and molecular function. D. The 20 most significant down-regulated pathways (LLPS vs DC). KEGG (Kyoto Encyclopedia of Genes and Genomes) pathway classification of target genes. Scatter diagram of enriched KEGG pathways of 20 differentially expressed genes. The Y-axis represents the name of pathway and the X-axis represents the Rich factor. The point size indicates the number of differentially expressed genes in one pathway, and the color of the point corresponds to the range of the Q value. NC: normal control group: DC: disease control group; LLPS: loquat leaf polysaccharide group.

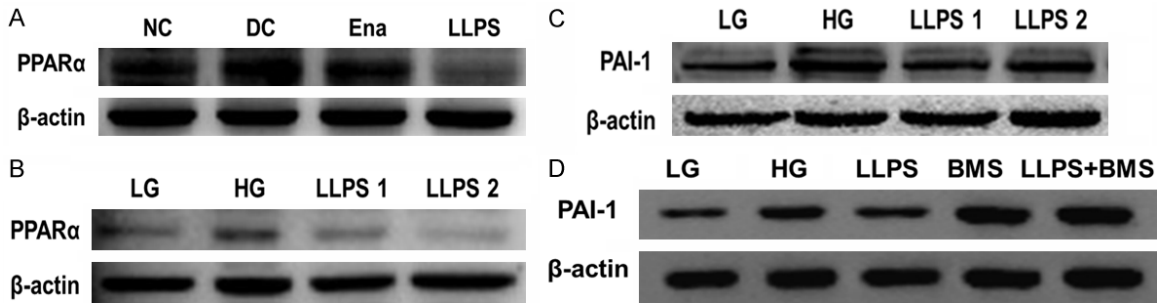


**Figure 5.** PPARα analyzed by western blot. A. Expression of PPARα in renal cortex. B-D. The expression of PPARα and PAI-1 in MMCs. LG: low glucose, HG: high glucose, LLPS 1: loquat leaf polysaccharide (50 μg/mL), LLPS 2: loquat leaf polysaccharide (100 μg/mL), BMS: BMS-687453 (426 nM).

shown in **Figure 5B**, LLPS reversed the up-regulation of PPARα induced by a high-glucose culture medium. Moreover, LLPS reversed the elevated PAI-1 expression in high-glucose culture medium (**Figure 5C**). Furthermore, we used BMS-687453, an agonist of PPARα, to check whether regulation of PPARα was associated with PAI-1 expression. We found that the levels of PAI-1 protein were down-regulated by LLPS treatment but de-suppressed by combining LLPS with PPARα agonist BMS-687453, thereby confirming that PPARα activity could directly affect PAI-1 expression (**Figure 5D**).

In summary, these results demonstrate that the PPARα signaling pathway was activated in anti-Thy 1 nephritis, which could be inhibited by LLPS treatment.

## Discussion

Loquat leaf is a type of Chinese medicine that has many pharmacological activities, such as suppressing coughs, lowering blood sugar, anti-inflammation, anti-tumor etc. [23, 41]. The main active components of loquat leaf include volatile oil, flavonoids, terpenoids, organic acids, etc., which have been proven to have anti-inflammatory, hypoglycemic, and anti-cancer effects by a large number of studies. In contrast, the effects of loquat leaf components on nephritis have not been reported. Polysaccharide extracts from Chinese medicine, such as astragalus polysaccharide, have been shown to improve chronic glomerulonephritis. One study shows that decocted loquat leaf had a clinically favorable curative effect in 80 cases of acute glomerulonephritis in children. However, it is not clear whether LLPS are active components in the treatment for protecting kidney function. We know that astragalus polysaccharide can improve C-BSA-induced glomerulonephritis in rats by suppressing NF-κB activation and NF-κB-regulated cytokine expressions [24]. Furthermore, Wang and coworkers illustrated that polysaccharide from *Irpex lacteus* (Fr.) Fr. efficiently inhibits membranous glomerulonephritis, possibly by targeting inflammation and NF-κB [25]. Therefore, we speculated that LLPS may be an effective component in the treatment of nephritis. Because there are few studies on the pharmacological effects of LLPS at present, our aim was to

explore the therapeutic effects of LLPS on chronic nephritis and decipher the potential mechanism.

We took advantage of a rat model of Thy-1 nephritis induced by the injection of anti-rat thymocyte serum to evaluate the function of LLPS [42]. Some common pathological phenomena have been observed in experimental glomerulonephritis, including massive proteinuria, increased expression of TGF-β, mesangial cell proliferation, and mesangial matrix expansion [43]. The rats in our model group showed significant elevated level of Cr and BUN and marked decreased level of Ccr compared with the NC group. LLPS-treated rats had a demonstrable reduction in BUN/Cr and an obvious increase in Ccr compared with untreated rats (**Table 1**; **Figure 1**). Although this trend of an increase in Ccr after LLPS treatment did not reach statistical significance, it suggests that the mechanism involved in LLPS for renoprotection is not completely dependent on its hemodynamic effects (**Figure 1**). In addition, the urinary protein excretion of the DC group continued to rise during the following 8 weeks, whereas LLPS treatment retarded the progressive increases of proteinuria in rats. Podocyte injury, the major cause of proteinuria in glomerular diseases, is characterized by capillary wall thickening and mesangial expansion due to increased matrix deposition and hypercellularity [44]. In this regard, we observed that the DC group showed mesangial cells proliferation, mesangial matrix hyperplasia, irregular basement membrane thickening, and foot process fusion compared to the NC group ($P<0.05$). Inspiringly, these changes were substantially ameliorated by treatment with LLPS. WT1, a nucleoprotein specific to adult renal foot cells and parietal glomerular epithelial cells, was dramatically decreased in disease rats. Conversely, LLPS treatment effectively restored WT1 expression (**Figure 2A-D**). In addition to reducing podocyte injury, LLPS also influenced renal fibrosis. Results of PAS staining showed that the glomeruli in the DC group had a remarkable accumulation of ECM compared to normal glomeruli. LLPS treatment improved the pathological changes of glomeruli, which was reflected in the scores of ECM in glomeruli. PAI-1 is closely associated with renal fibrosis and its elevation leads to reduced ECM degradation. As expected, the expression of PAI-1 in DC rats was significantly higher than that in normal rats. Interestingly, LLPS treatment also reversed the expression of PAI-1 (**Figure 3A-C**). Thus, we demonstrated that LLPS protects podocytes and inhibits renal fibrosis in rats with anti-Thy 1 nephritis.

Comparison of the protective effect of LLPS on nephritis with that of Ena (for which the active metabolite is an angiotensin-converting-enzyme inhibitor that could cause less vasoconstriction and decreased blood pressure [45]), shows that LLPS had a comparable cure effect for decreasing urinary protein (**Figure 1**) and improving podocyte injury (**Figure 2A-D**) and renal fibrosis (**Figure 3A-C**). In detail, LLPS treatment reduced plasma BUN by 28% and 24-h proteinuria by 76% after 8 weeks. Furthermore, LLPS treatment improved podocyte injury by reducing glomerular basement membrane thickness by 28% and foot processes width by 35%, and improved renal fibrosis by decreasing glomerular matrix expansion by 45%. Therefore, LLPS treatment might be a promising protective therapy for chronic glomerulonephritis with few side effects.

To reveal the potential mechanism of LLPS treatment, we applied RNA-seq to expand our investigation. The RNA-seq analysis showed that 504 up-regulated genes and 297 down-regulated genes were significantly differentially expressed between LLPS and DC groups. Pathway enrichment analysis indicated that the most significant pathways involving these differential genes include the PPAR signaling pathway, which is evidently up-regulated in the DC group compared to the LLPS group. PPARs belong to the steroid hormone receptor superfamily, and there are three PPAR subtypes; namely, PPARα, PPARβ/δ, and PPARγ. Of these subtypes, PPARα is closely related to nephritis in many studies [46-49]. Therefore, we tested the PPARα pathway of LLPS treatment in mesangial cell fibrosis *in vitro*. Consist with the results *in vivo*, the data collected from cell experiments demonstrate that LLPS suppressed PPARα signaling pathway *in vitro*. To validate the finding that PPARα activation stimulated PAI-1 expression, we used an agonist of PPARα (BMS-687453) to stimulate PPARα activity, and then examined the expression of PAI-1 by western blotting. We found that the down-regulated PAI-1 effect by LLPS treatment could be de-suppressed by combining LLPS with PPARα agonist BMS-687453, thus con-

firming that PPARα could directly affect PAI-1 expression. In light of these findings, we suggest that LLPS treatment suppresses the expression of fibrosis factor PAI-1 partially via PPARα inhibition. It is of interest that PPAR has been reported to display important roles of reducing pain and inflammation, inducing oxidative stress and lipidomic remodeling, and enhancing inflammation in gout arthritis [50], liver enlargement [51], and endometritis, respectively [52]. Also, Koji Hashimoto and coworkers suggest that PPARα-related medicines might act as a treatment option for CKD [48]. In our study, we confirmed that inhibition of PPARα by LLPS treatment improved podocyte injury and inhibited glomerular fibrosis in rats with anti-Thy 1 nephritis.

## Conclusions

Our results show that LLPS could protect kidney function by inhibiting ECM accumulation and ameliorating glomerular damage in experimental anti-Thy1-induced glomerulonephritis. The mechanism of these effects may involve suppression of the PPARα signaling pathway. Our findings have the potential of leading to development of a new strategy of protection therapy for chronic glomerulonephritis.

## Acknowledgements

This work was supported by the National Natural Science Foundation of China 81670200, 81770220, 81600177 (to YY & CG); the 2016 Outstanding Youth Fund of Jiangsu Province BK20160048 (to YY); the Natural Science Foundation of Jiangsu Province BK20161041 (to CG); the National key research and development program-precision medicine sub-program 2016YFC0905900 (to YY); The Priority Academic Program Development of Jiangsu Higher Education Institutions for Chinese Medicine; and the Innovation Team of Six Talent Peaks Project in Jiangsu Province TD-SWYY-015 (to CG).

## Disclosure of conflict of interest

None.

**Address correspondence to:** Chunyan Gu, The Third Affiliated Hospital of Nanjing University of Chinese Medicine, Nanjing 210001, China. Tel: (86) 25858-11597; E-mail: guchunyan@njucm.edu.cn; Ye Yang, School of Medicine and Life Sciences, Nanjing University of Chinese Medicine, Nanjing 210023, China. E-mail: yangye876@sina.com; Jianming Ju, Affiliated Hospital of Integrated Traditional Chinese and Western Medicine, Nanjing University of Chinese Medicine, Nanjing, China. E-mail: jjm405@126.com

## References

[1] Franca Gois PH, Wolley M, Ranganathan D and Seguro AC. Vitamin D deficiency in chronic kidney disease: recent evidence and controversies. Int J Environ Res Public Health 2018; 15.
[2] Levey AS, Coresh J. Chronic kidney disease. Lancet 2012; 379: 165-80.
[3] Demirjian S, Lane BR, Derweesh IH, Takagi T, Fergany A and Campbell SC. Chronic kidney disease due to surgical removal of nephrons: relative rates of progression and survival. J Urol 2014; 192: 1057-1062.
[4] Li YK, Ma DX, Wang ZM, Hu XF, Li SL, Tian HZ, Wang MJ, Shu YW and Yang J. The glucagon-like peptide-1 (GLP-1) analog liraglutide attenuates renal fibrosis. Pharmacol Res 2018; 131: 102-111.
[5] Yanagita M. Inhibitors/antagonists of TGF-beta system in kidney fibrosis. Nephrol Dial Transplant 2012; 27: 3686-3691.
[6] Hundae A and McCullough PA. Cardiac and renal fibrosis in chronic cardiorenal syndromes. Nephron Clin Pract 2014; 127: 106-112.
[7] Zhong X, Tu YJ, Li Y, Zhang P, Wang W, Chen SS, Li L, Chung AC, Lan HY, Chen HY, Li GS, Wang L. Serum levels of WANT-inducible signaling pathway protein-1 (WISP-1): a noninvasive biomarker of renal fibrosis in subjects with chronic kidney disease. Am J Transl Res 2017; 9: 2920-2932.
[8] Fanelli C, Delle H, Cavaglieri RC, Dominguez WV and Noronha IL. Gender differences in the progression of experimental chronic kidney disease induced by chronic nitric oxide inhibition. Biomed Res Int 2017; 2017: 2159739.
[9] Hou X, Tian J, Geng J, Li X, Tang X, Zhang J, Bai X. MicroRNA-27a promotes renal tubulointerstitial fibrosis via suppressing PPARγ pathway in diabetic nephropathy. Oncotarget 2016; 7: 47760-47776.
[10] Zhou J, Chen Y, Liu Y, Shi S, Wang S, Li X, Zhang H and Wang H. Urinary uromodulin excretion predicts progression of chronic kidney disease resulting from IgA nephropathy. PLoS One 2013; 8: e71023.
[11] Fu J, Lee K, Chuang PY, Liu Z and He JC. Glomerular endothelial cell injury and cross talk in diabetic kidney disease. Am J Physiol Renal Physiol 2015; 308: F287-297.
[12] Tung CW, Hsu YC, Shih YH, Chang PJ and Lin CL. Glomerular mesangial cell and podocyte injuries in diabetic nephropathy. Nephrology 2018; 23: 32-37.

[13] Liu M, Liang K, Zhen J, Zhou M, Wang X, Wang Z, Wei X, Zhang Y, Sun Y, Zhou Z, Su H, Zhang C, Li N, Gao C, Peng J and Yi F. Sirt6 deficiency exacerbates podocyte injury and proteinuria through targeting Notch signaling. Nat Commun 2017; 8: 413.
[14] Li PK, Kwan BC, Chow KM, Leung CB and Szeto CC. Treatment of early immunoglobulin A nephropathy by angiotensin-converting enzyme inhibitor. Am J Med 2013; 126: 162-168.
[15] Liu M, Park J, Wu X, Li Y, Tran Q, Mun K, Lee Y, Hur GM, Wen A and Park J. Shen-Kang protects 5/6 nephrectomized rats against renal injury by reducing oxidative stress through the MAPK signaling pathways. Int J Mol Med 2015; 36: 975-984.
[16] Lu Z, Zeng Y, Lu F, Liu X and Zou C. Rhubarb enema attenuates renal tubulointerstitial fibrosis in 5/6 nephrectomized rats by alleviating indoxyl sulfate overload. PLoS One 2015; 10: e0144726.
[17] Qiu H, Fan W, Fu P, Zuo C, Feng P, Liu F, Zhou L, Chen F, Zhong H, Liang Y and Shi M. General acteoside of rehmanniae leaves in the treatment of primary chronic glomerulonephritis: a randomized controlled trial. Afr J Tradit Complement Altern Med 2013; 10: 109-15.
[18] Qiu H, Fu P, Fan W, Zuo C, Feng P, Shi P, Cao L, Liu F, Zhou L, Chen F, Zhong H, Gou Z, Liang Y and Shi M. Treatment of primary chronic glomerulonephritis with Rehmannia glutinosa acteosides in combination with the angiotensin receptor blocker irbesartan: a randomized controlled trial. Phytother Res 2014; 28: 132-136.
[19] Wan YG, Che XY, Sun W, Huang YR, Meng XJ, Chen HL, Shi XM, Tu Y, Wu W and Liu YL. Low-dose of multi-glycoside of Tripterygium wilfordii Hook. f., a natural regulator of TGF-beta1/Smad signaling activity improves adriamycin-induced glomerulosclerosis in vivo. J Ethnopharmacol 2014; 151: 1079-1089.
[20] Mungun HK, Li S, Zhang Y, Huang S, Jia Z, Ding G, Zhang A. Dihydroartemisinin inhibits indoxyl sulfate (IS)-promoted cell cycle progression in mesangial cells by targeting COX-2/mPGES-1/PGE2 cascade. Am J Transl Res 2018; 10: 422-431.
[21] Oliveira T. Anti-inflammatory and antinociceptive effects of the aqueous extract of the bark of chrysobalanus icaco Linnaeus. British Journal of Pharmaceutical Research 2014; 4: 1253-1268.
[22] Choi YG, Seok YH, Yeo S, Jeong MY and Lim S. Protective changes of inflammation-related gene expression by the leaves of Eriobotrya japonica in the LPS-stimulated human gingival fibroblast: microarray analysis. J Ethnopharmacol 2011; 135: 636-645.
[23] Cha DS, Eun JS and Jeon H. Anti-inflammatory and antinociceptive properties of the leaves of Eriobotrya japonica. J Ethnopharmacol 2011; 134: 305-312.
[24] Ji L, Chen X, Zhong X, Li Z, Yang L, Fan J, Tang W, Qin W. Astragalus membranaceus up-regulate Cosmc expression and reverse IgA dysglycosylation in IgA nephropathy. BMC Complement Altern Med 2014; 14: 195.
[25] Wang J, Song J, Wang D, Zhang N, Lu J, Meng Q, Zhou Y, Wang N, Liu Y, Wang D and Teng L. The anti-membranous glomerulonephritic activity of purified polysaccharides from Irpex lacteus Fr. Int J Biol Macromol 2016; 84: 87-93.
[26] Wang C Q CJ, Cheng Y, Huang L, Wang Z. Study on preparation of salidroside and polysaccharide in Rhodiola crenulata. Zhong Yao Cai 2011; 34: 1122-1125.
[27] Lv X, Wang C, Cheng Y, Huang L and Wang Z. Isolation and structural characterization of a polysaccharide LRP4-A from lycium ruthenicum Murr. Carbohydr Res 2013; 365: 20-25.
[28] Xie LY, Zhang Y, Peng WH, Gan BC. Study on methods of deproteinization from phellinus baumii polysaccharide. Zhong Yao Cai 2011; 34: 293-295.
[29] Zhang HL, Cui SH, Zha XQ, Bansal V, Xue L, Li XL, Hao R, Pan LH and Luo JP. Jellyfish skin polysaccharides: extraction and inhibitory activity on macrophage-derived foam cell formation. Carbohydr Polym 2014; 106: 393-402.
[30] He YM, Feng L, Huo DM, Yang ZH and Liao YH. Enalapril versus losartan for adults with chronic kidney disease: a systematic review and meta-analysis. Nephrology (Carlton) 2013; 18: 605-614.
[31] Dowling TC, Wang ES, Ferrucci L and Sorkin JD. Glomerular filtration rate equations overestimate creatinine clearance in older individuals enrolled in the Baltimore longitudinal study on aging: impact on renal drug dosing. Pharmacotherapy 2013; 33: 912-921.
[32] Ye EA and Steinle JJ. miR-146a suppresses STAT3/VEGF pathways and reduces apoptosis through IL-6 signaling in primary human retinal microvascular endothelial cells in high glucose conditions. Vision Res 2017; 139: 15-22.
[33] Keon-Cheol Lee JSL, Sunhyo Jo, DaeHee Kim, Sang Youb Han. High glucose induces inflammatory reactions and changes in histonemodifying enzymes in rat mesangial cells. Biomedical Research 2018; 29: 1103-1109.
[34] Zhang R, Li J, Huang T, Wang X. Danggui buxue tang suppresses high glucose-induced proliferation and extracellular matrix accumulation of mesangial cells via inhibiting lncRNA PVT1. Am J Transl Res 2017; 9: 3732-3740.
[35] Du YG, Wang LP, Qian JW, Zhang KN and Chai KF. Panax notoginseng saponins protect kid-

ney from diabetes by up-regulating silent information regulator 1 and activating antioxidant proteins in rats. Chin J Integr Med 2016; 22: 910-917.
[36] Hu Q, Yang C, Wang Q, Zeng H and Qin W. Demethylzeylasteral (T-96) treatment ameliorates mice lupus nephritis accompanied by inhibiting activation of NF-kappaB pathway. PLoS One 2015; 10: e0133724.
[37] Zhou H, Kajiyama H, Tsuji T, Hu X, Leelahavanichkul A, Vento S, Frank R, Kopp JB, Trachtman H, Star RA and Yuen PS. Urinary exosomal Wilms' tumor-1 as a potential biomarker for podocyte injury. Am J Physiol Renal Physiol 2013; 305: F553-559.
[38] Olea-Herrero N, Arenas MI, Munoz-Moreno C, Moreno-Gomez-Toledano R, Gonzalez-Santander M, Arribas I and Bosch RJ. Bisphenol-A induces podocytopathy with proteinuria in mice. J Cell Physiol 2014; 229: 2057-2066.
[39] Liu N, Zhang Y, Su H, Wang J, Liu Z and Kong J. Effects of cholecalciferol cholesterol emulsion on renal fibrosis and aquaporin 2 and 4 in mice with unilateral ureteral obstruction. Biomed Pharmacother 2018; 102: 633-638.
[40] Brocker CN, Patel DP, Velenosi TJ, Kim D, Yan T, Yue J, Li G, Krausz KW, Gonzalez FJ. Extrahepatic PPARα modulates fatty acid oxidation and attenuates fasting-induced hepatosteatosis in mice. J Lipid Res 2018; 59: 2140-2152.
[41] Tamaya K, Matsui T, Toshima A, Noguchi M, Ju Q, Miyata Y, Tanaka T and Tanaka K. Suppression of blood glucose level by a new fermented tea obtained by tea-rolling processing of loquat (Eriobotrya japonica) and green tea leaves in disaccharide-loaded Sprague-Dawley rats. J Sci Food Agric 2010; 90: 779-783.
[42] Yoshimura A, Gordon K, Alpers CE, Floege J, Pritzl P, Ross R, Couser WG, Bowen-Pope DF and Johnson RJ. Demonstration of PDGF B-chain mRNA in glomeruli in mesangial proliferative nephritis by in situ hybridization. Kidney International 1991; 40: 470-476.
[43] Cheng QL, Orikasa M, Morioka T, Kawachi H, Chen XM, Oite T, Shimizu F. Progressive renal lesions induced by administration of monoclonal antibody 1-22-3 to unilaterally nephrectomized rats. Clin Exp Immunol 1995; 102: 181-185.
[44] Cook HT and Pickering MC. Histopathology of MPGN and C3 glomerulopathies. Nat Rev Nephrol 2015; 11: 14-22.
[45] Juhlin T, Erhardt LR, Ottosson H, Jonsson BA and Hoglund P. Treatments with losartan or enalapril are equally sensitive to deterioration in renal function from cyclooxygenase inhibition. Eur J Heart Fail 2007; 9: 191-196.
[46] Youssef J and Badr MZ. PPARs: history and advances. Methods Mol Biol 2013; 952: 1-6.
[47] Kamijo Y, Hora K, Nakajima T, Kono K, Takahashi K, Ito Y, Higuchi M, Kiyosawa K, Shigematsu H, Gonzalez FJ and Aoyama T. Peroxisome proliferator-activated receptor alpha protects against glomerulonephritis induced by long-term exposure to the plasticizer di-(2-ethylhexyl)phthalate. J Am Soc Nephrol 2007; 18: 176-188.
[48] Hashimoto K, Kamijo Y, Nakajima T, Harada M, Higuchi M, Ehara T, Shigematsu H and Aoyama T. PPARalpha activation protects against anti-Thy1 nephritis by suppressing glomerular NF-kappaB signaling. PPAR Res 2012; 2012: 976089.
[49] Gomez IG, MacKenna DA, Johnson BG, Kaimal V, Roach AM, Ren S, Nakagawa N, Xin C, Newitt R, Pandya S, Xia TH, Liu X, Borza DB, Grafals M, Shankland SJ, Himmelfarb J, Portilla D, Liu S, Chau BN and Duffield JS. Anti-microRNA-21 oligonucleotides prevent Alport nephropathy progression by stimulating metabolic pathways. J Clin Invest 2015; 125: 141-156.
[50] Ruiz-Miyazawa KW, Staurengo-Ferrari L, Pinho-Ribeiro FA, Fattori V, Zaninelli TH, Badaro-Garcia S, Borghi SM, Andrade KC, Clemente-Napimoga JT, Alves-Filho JC, Cunha TM, Fraceto LF, Cunha FQ, Napimoga MH, Casagrande R and Verri WA Jr. 15d-PGJ2-loaded nanocapsules ameliorate experimental gout arthritis by reducing pain and inflammation in a PPAR-gamma-sensitive manner in mice. Sci Rep 2018; 8: 13979.
[51] Ament Z, West JA, Stanley E, Ashmore T, Roberts LD, Wright J, Nicholls AW and Griffin JL. PPAR-pan activation induces hepatic oxidative stress and lipidomic remodelling. Free Radic Biol Med 2016; 95: 357-368.
[52] Socha BM, Lada P, Szczepanska AA, Lupicka M and Korzekwa AJ. The influence of experimentally induced endometritis on the PPAR expression profile in the bovine endometrium. Theriogenology 2018; 122: 74-83.